Design Strategy for Monolithically Integrated Photodetector and Improvement using Plasmonics

Q. Ding, S. Sant, and A. Schenk

Integrated Systems Laboratory, ETH Zurich
Zurich, 8092, Switzerland
dingq@iis.ee.ethz.ch, ssant@iis.ee.ethz.ch, schenk@iis.ee.ethz.ch

***Abstract*—We report three optimized coupling geometries for a monolithically integrated $In_{0.53}Ga_{0.47}As$ pin photodetector operating at 1350 nm wavelength. It is shown how plasmonics can further improve the performance.**

I. Introduction

Waveguide-coupled photodetectors with high quantum efficiency and cutoff frequency are key components in photonic integrated circuits. The state-of-art coupling approach is heterogeneous integration, where a photodetector is vertically coupled to a waveguide buried underneath [1]. The recently developed Template Assisted Selective Epitaxy (TASE) technology [2] enables monolithic integration of III-V materials on a Si platform. This allows arranging both the waveguide and the photodetector on top of the SiO_2 substrate and coupling them horizontally.

In this work, we present three horizontal coupling geometries with device performance optimized using 3D optoelectrical simulations and explore the potential improvement by introducing plasmonics.

II. Coupling Geometries

The three proposed coupling geometries are sketched in Fig. 1. In all cases, light propagates along the waveguide and couples to the photodetector, which has the same height and width as the waveguide. For side coupling, the light propagation direction is perpendicular to the carrier transport direction, whereas these two directions are parallel in the case of butt coupling.

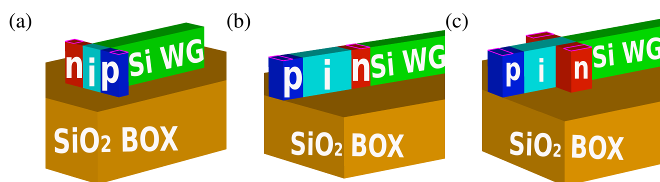

Fig. 1: Structures with (a) side coupling, (b) butt coupling without offshoot, (c) butt coupling with n-offshoots.

III. Structure Optimization

Two structure parameters are crucial for design optimization in this study. One is the waveguide height, which determines the mode formation within the waveguide. Considering miniaturization, it should be as small as possible but sufficient for mode formation. The other is the photodetector i-region length along the propagation direction. It impacts mode distribution in the i-region, carrier transit time, and junction capacitance, thus should be optimized for device performance. The remaining geometry parameters of photodetector and waveguide are all set to 200 nm.

A. Minimizing Waveguide Height

The study of mode formation within the waveguide is performed using *Lumerical Mode Solver*. The simulated system is a Si waveguide on top of a SiO_2 substrate. A mode confinement factor is used to quantify the mode formation, which is defined as the fraction of field energy confined within the waveguide with respect to the entire simulation region. Simulations are performed by sweeping the waveguide height from 60 nm to 500 nm.

Fig. 2(a). shows that the TM mode starts to form as the height reaches 110 nm and that it dominates beyond 180 nm. At small height (Fig. 2(b)) the mode is strongly leaked into the oxide. As the height increases (Fig. 2(c)), the mode starts to form within the waveguide. The minimum height for sufficient TM mode formation is found to be 240 nm, which is extracted based on -3dB of the saturated confinement factor (as a function of height). The waveguide height is fixed to this value in the following optimization step.

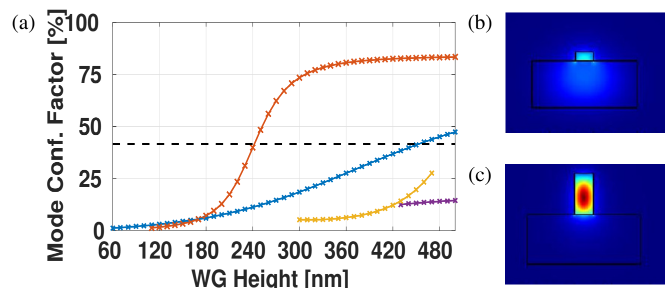

Fig. 2: (a) Plot of mode confinement factor vs. waveguide height, with blue curve for TE mode (E polarization fraction > 90%), red curve for TM mode (E polarization fraction < 10%), yellow (purple) curve for mixed mode with E polarization fraction between 20% - 25% (80% - 90%) and black dashed curve as -3dB conf. factor for TM mode; TM mode field power distribution at height of (b) 110 nm and (c) 420 nm.

978-1-7281-1647-1/19/$31.00 ©2019 IEEE

B. Optimization of Photodetector i-region Length

The optimal photodetector i-region length (Li) is deduced considering the trade-off between three performance parameters, including max. internal quantum efficiency (IQE), optical and electrical cutoff frequency. These are obtained from optical and electrical AC analysis using *Sentaurus Device* with the optical generation rate profile from FDTD simulations as input. The studied frequency range is from 10 kHz to 100 THz, and the photodetector is reverse biased at 2V.

For side coupling, Li is swept from 500 nm to 40 nm. Simulations show that the highest max. IQE and optical cutoff frequency appears at 100 nm, which indicates that the mode is strongly confined within the i-region for this length. The electrical cutoff frequency always increases as Li decreases. This is because Li is proportional to the capacitance in this structure. Considering the trade-off between optical and electrical performance, 100 nm is chosen as the optimal Li.

For both butt coupling structures, Li is swept from 700 nm to 300 nm. In the case of butt coupling without offshoots, a contact metal is added on top of the n-region in order to take into account the effect of light absorption by the metal. Results show that as Li decreases, the max. IQE decreases as result of the reduced light absorption, but the optical cutoff frequency increases because of the shorter carrier transit time. For butt coupling with n-offshoots, due to the complicated geometry, no monotonic tendency in the optical behavior is observed. The electrical cutoff frequency always decreases as Li decreases in both cases, since here Li is inversely proportional to the capacitance. The final optimal Li in both structures is found to be 500 nm.

C. Structure with Best Coupling

Comparing the performance of the three optimized structures, Fig. 3(a) shows that butt coupling with n-offshoots has the highest max. IQE, but its optical cutoff frequency is one order of magnitude lower than for side coupling. Butt coupling without offshoots has the worst optical performance due to the influence of the contact metal on the n-region. The difference in the electrical behavior between the three structures is negligible, as shown in Fig. 3(b).

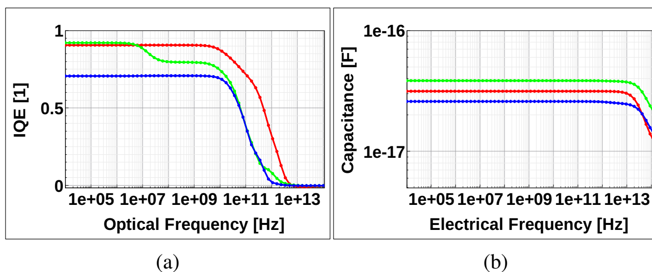

(a) (b)

Fig. 3: (a) Optical and (b) electrical behavior of three optimized structures, with red curve for side coupling and green (blue) curve for butt coupling with (without) n-offshoots.

Therefore, the side coupling structure provides the optimal device performance with the smallest device size. The performance parameters of the three optimized structures are summarized in Table 1, where the cutoff frequencies are obtained from the -3dB line of the curves shown in Fig. 3.

TABLE I: Device performance of three optimized structures.

	max. IQE [%]	*opt. cutoff freq. [GHz]*	*ele. cutoff freq. [THz]*
side coupling	91	800	30
butt coupling without offshoots	71	100	70
butt coupling with n-offshoots	93	70	60

IV. Improvement by Plasmonics

The low optical cutoff frequency of the butt coupling structure with n-offshoots originates from the low electric field in the unbiased i-region between the two n-offshoots. To overcome this drawback, two Ag rods are added on top of the i-region, as sketched in Fig. 4 (a). Fig. 4 (b) shows that light couples to one plasmonic mode formed at the metal corners near the metal/i-region interface. As the metal flattens the potential, the electric field in the unbiased i-region between the two offshoots is significantly enhanced (Fig. 4(d)), compared to the structure without Ag rods (Fig. 4(c)). This leads to a remarkable improvement of the optical cutoff frequency from 70 GHz (without Ag rods) to 300 GHz.

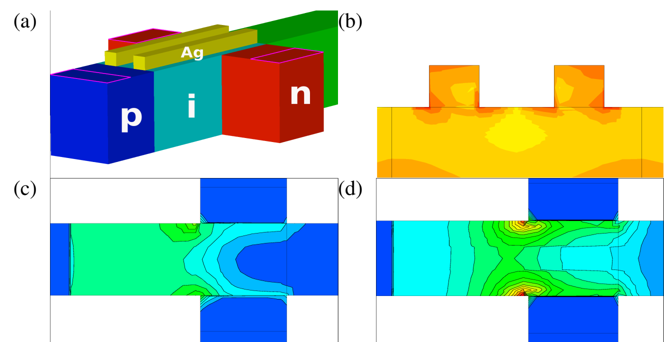

Fig. 4: (a) 60 nm-spaced double 40x40 nm Ag rods on top of i-region in butt coupling structure with n-offshoots, (b) optical generation rate profile along n-i-n direction cut; E-field in i-region of structure (c) without Ag and (d) with Ag, with color scale range from 1.928e-05 V/cm to 2.218e+05 V/cm.

Conclusion

The side coupling structure turns out to be the best design among three proposed coupling geometries, in terms of scalability and device performance. Furthermore, plasmonics significantly improves the performance of the butt coupling structure with n-offshoots, making it more compatible with the side coupling structure.

References

[1] Nannicha,H. Alban,G. and Laurent,C., "Heterogeneous integration of GaInAsSb p-i-n photodiodes on a Silicon-on-Insulator waveguide circuit," IEEE Photonics Technology Letters, vol. 23, pp.1760-1762, 2011
[2] Schmid,H. Borg,M. and Moselund,K., "Template-assisted selective epitaxy of IIIV nanoscale devices for co-planar heterogeneous integration with Si," Applied Physics Letters, vol. 106, pp.233101, 2015.